

# A computational perspective of molecular interactions through virtual screening, pharmacokinetic and dynamic prediction on ribosome toxin A chain and inhibitors of *Ricinus communis*

R. Barani Kumar, M. Xavier Suresh

Department of Bioinformatics, Sathyabama University, Chennai, Tamil Nadu, India

Submitted: 25-07-2011

Revised: 04-09-2011

Published: 22-12-11

## ABSTRACT

**Background:** Ricin is considered to be one of the most deadly toxins and gained its favor as a bioweapon that has a serious social and biological impact, due to its widespread nature and abundant availability. The hazardous effects of this toxin in human being are seen in almost all parts of the organ system. The severe consequences of the toxin necessitate the need for developing potential inhibitors that can effectively block its interaction with the host system. **Materials and Methods:** In order to identify potential inhibitors that can effectively block ricin, we employed various computational approaches. In this work, we computationally screened and analyzed 66 analogs and further tested their ADME/T profiles. From the kinetic and toxicity studies we selected six analogs that possessed appropriate pharmacokinetic and dynamic property. We have also performed a computational docking of these analogs with the target. **Results:** On the basis of the dock scores and hydrogen bond interactions we have identified analog 64 to be the best interacting molecule. Molecule 64 seems to have stable interaction with the residues Tyr80, Arg180, and Val81. The pharmacophore feature that describes the key functional features of a molecule was also studied and presented. **Conclusion:** The pharmacophore features of the drugs provided suggests the key functional groups that can aid in the design and synthesis of more potential inhibitors.

**Key words:** Benzocaine, ligand fit, pharmacophore, ricin, virtual screening

## INTRODUCTION

Ricin, also called RCA-II or RCA60, is a toxic protein found within the beans of the castor plant (*Ricinus communis*). Ricin causes various allergic reactions and toxicity; however, the severity depends on the route of entry. Ricin poisoning can occur *via* injection, inhalation, or ingestion, of which the latter two are considered to be the most lethal routes of exposure.<sup>[1]</sup> The exposure to ricin extends its effects to various organs of the organism and is pathologically influenced particularly by the liver, kidneys, lymph nodes, and lungs. Moreover, it causes hyperpyrexia and interacts with the electrolyte and hormone metabolism as well.<sup>[2]</sup> Low doses can lead to progressive and diffuse pulmonary

edema with associated inflammation and necrosis of the alveolar pneumocytes.<sup>[3]</sup> Ricin's widespread availability makes it a viable biological weapon.<sup>[4]</sup> As an agent of terror, it could be used to contaminate an urban water supply, with the intent of causing lethality in a large urban population and also by exposure to toxin contaminated food and air.<sup>[3]</sup> Ricin toxin gained its fame by its use in the so-called "umbrella murder" to kill the Bulgarian dissident Georgi Markov in 1978.<sup>[5,6]</sup> As little as 500  $\mu\text{m}$  can kill an adult.<sup>[5]</sup> Studies on mouse models of ricin toxication indicated a characteristic symptom of hemolytic uremic syndrome, including thrombotic microangiopathy, hemolytic anemia, thrombocytopenia, and acute renal failure,<sup>[7]</sup> when applied to eyes, ricin causes inflammation of the eyes and adnexa.<sup>[8]</sup> On the other hand, oxidative gross measurement shows that it has no antifilarial effect.<sup>[9]</sup>

Ricin is a potent ribotoxin belonging to RIP (ribosome inactivating protein) II type lectin family having 28S

### Access this article online

**Website:**

[www.phcogres.com](http://www.phcogres.com)

**DOI:**

10.4103/0974-8490.91027

**Quick Response Code:****Address for correspondence:**

R. Barani Kumar, Department of Bioinformatics, Sathyabama University, Rajiv Gandhi Road, Jeppiaar Nagar, Chennai 600 119, Tamil Nadu, India. E-mail: [baranisathyabama@gmail.com](mailto:baranisathyabama@gmail.com)

rRNA of the 60S ribosomal subunit as its cytosolic target.<sup>[10,11]</sup> Its ribotoxic actions lead to the inhibition of protein synthesis by inhibiting the translation upon removal of specific adenine from 28S RNA and also inhibit the phosphorylation of stress-activated protein kinases (SAPKs).<sup>[12,13]</sup> The ricin gene family encodes three domains: an N-terminal RIP domain and two C-terminal lectin domains. The draft sequence contains 28 putative genes of the lectin family of which seven encode proteins that contain RIP and the two lectin domains, nine encode proteins with only RIP domain, and nine encode proteins with one or two lectin domains only.<sup>[14]</sup>

The toxin is a dimeric protein consisting of an enzymic A chain (the toxic subunit) and a B chain with lectin properties aiding the uptake of the whole molecule into cells through cell binding.<sup>[15]</sup> The A chain of ricin (RA) is a cytotoxic RNA N-glycosidase that inactivates ribosomes by depurination of the adenosine residue at position 4324 in 28S rRNA.<sup>[16]</sup> The ricin-A chain consists of two forms which differ in sugar content. The major component A1 contains one high mannose chain while the minor component A2 contains an additional high mannose chain.<sup>[17]</sup>

The toxin, which consists of two polypeptide chains, binds only by the B chain to both glycolipids and glycoproteins with terminal galactose at the cell surface receptors followed by which the A-chain enters the cytosol and inhibits protein synthesis enzymatically. The toxin follows a retrograde transport route. After binding the toxin is endocytosed by different mechanisms, it is transported *via* endosomes to the golgi apparatus and the endoplasmic reticulum (ER).<sup>[18,19]</sup> Recent evidence suggests that ricin binds to galactosylated calreticulin, which may carry the toxin from the Golgi apparatus to the ER. Ricin is perceived to be a candidate for ER-associated degradation, but a fraction of the ricin survives and is translocated to cytoplasm where it inhibits protein synthesis by inactivating ribosomes, ultimately leading to cell death.<sup>[20,21]</sup>

The detailed process of cellular entry and ribosome inactivation is explained by Liu *et al.*<sup>[22]</sup> This studies report that ricin toxicity apart from inhibiting protein synthesis also induces apoptosis of immune cells and plays an important role in intestinal injury. Scientists have identified about 28 different proteins of the brush border membranes of *Intestinal villi* to interact with the toxin, substantiating the reason for the intensive toxicity in the intestine.<sup>[22]</sup> Its immunological action is well studied in macrophages, microglial cells, and other immune cells. Ricin is taken up by two routes in macrophages (i) by binding to cell surface mannose receptors, or (ii) by binding of the ricin galactose receptor to cell surface glycoproteins.<sup>[23]</sup> Macrophages show a high preference for the A2 component of ricin-A

chain.<sup>[17]</sup> Microglial cells, such as macrophages, are very sensitive to ricin. An evaluation of ricin uptake *via* both pathways analyzed in microglial cell lines in the presence and absence of lactose and mannose reported that all cultures were protected from toxicity more by lactose than mannose.<sup>[24]</sup> The protective nature of lactose was also confirmed recently by a group of scientists who tested the binding affinity of ricin in a lactose-incorporated polyacrylamide-based glycopolymers. It was observed that the glycopolymers effectively interfered with the toxin-lactoside adhesion event. Thus lactose is considered as a natural inhibitor of this toxin.<sup>[25]</sup> The impact of glycoprotein in the adhesion of ricin for its retrograde transport is well studied and a large number of reports have explained the crucial role of polymers in the ricin pathway. Contrarily glycosphingolipids had no effect on the transport of the toxin. When tested the transport of the toxin on a glycosphingolipid-deficient mouse melanoma cell line, in the same cell line transfected with ceramide glucosyltransferase to restore glycosphingolipid synthesis and in the parental cell line, the ricin transported retrogradely to the Golgi apparatus, the ER and translocated to the cytosol equally well and apparently at the same rate in cells with and without glycosphingolipids. However, depletion in cholesterol levels reduced the transport. Hence, it is well clear that glycosphingolipids do not contribute to the toxication of ricin toxin.<sup>[26]</sup>

Although several plant products are reported to have anti-cancer agents<sup>[27]</sup> ricin in recent years has been exploited for its anticancer activity. Investigation with human cervical cancer cell line HeLa indicated a ricin-induced cell death by the generation of reactive oxygen species.<sup>[28,29]</sup> Evaluation of its anticancer activity indicated that ricin is able to kill tumor cells selectively at low concentration, but the selectivity does not appear at high concentrations.<sup>[30]</sup> The mechanism of the toxic action is currently studied for the preparation of selective immunotoxins (ITs), which could be used in the therapy of various cancer diseases or HIV infection.<sup>[10]</sup> ITs consist of cell binding ligands coupled to toxins or their subunits.<sup>[31]</sup> Strategies utilizing ITs to target tumor cells surviving conventional treatment have attracted scientific and clinical interest.<sup>[32]</sup> Ricin is a promising candidate for the treatment of cancer because it can be selectively targeted to tumor cells via linkage to monoclonal antibodies.<sup>[32,33]</sup> The importance of herbal medicine and increasing stability of natural medicines are recently reviewed.<sup>[34]</sup>

In spite of its beneficiary effect as an anti-tumor agent, the toxicity profile of ricin cannot be overlooked. Research into the mechanism of toxicity, as well as strategies for treatment and protection from the toxin has been widely undertaken for a number of years. No specific treatment

or therapy is available for ricin poisoning or prevention. Studies on an insertional mutagenesis of a 25 residue internal peptide into ricin A chain reduced its activity by 300-fold. Rats when treated with the mutated toxin were found to be ricin-resistant and they developed a good titre of antiricin antibodies. Structural analysis of the toxin also reveals a probable method for developing anti-ricin vaccines.<sup>[35,36]</sup> Monoclonal antibodies developed against ricin also had a positive effect in inhibiting ricin-mediated cytotoxicity.<sup>[37,38]</sup> Bai *et al.* used computational studies and virtual screening as a method to identify potential inhibitors of the toxin.<sup>[39]</sup> They were able to identify two compounds that show moderate-to-strong inhibition, however showed cytotoxicity. With a well-characterized structure, the scientists believe that computational studies and virtual screening can contribute largely in the search of anti-ricin inhibitors.<sup>[40]</sup>

Docking various ligands to the protein of interest followed by scoring to reveal the strength of interaction and to determine the affinity of binding has become increasingly important in the context of drug discovery.<sup>[41,42]</sup> In this paper, we have employed a virtual screening approach to identify possible ricin inhibitors from a set of analogs screened from the Pubchem database and Zinc database. We performed a molecular docking of the selected analogs against ricin using Discovery Studio 2.0. Docking scores were used to identify the best interacting analogs and the pharmacophore models of the ligands were generated.

## MATERIALS AND METHODS

### Selection of biological data

The crystallographic structure of Ricin A chain complexed with formycin monophosphate (FMP) and adenylyl (3'->5') guanosine (1APG) was selected as the target for the study.<sup>[43]</sup> The 3D coordinates of the target with the PDB code 1APG was retrieved from protein data bank (PDB). Before docking all the hetero atoms and any water molecules associated with the protein were removed. The structure was minimized with conjugate gradient to resolve steric clashes and to remove unwanted interactions.

### Binding site analysis

Binding sites are cavities that are present in the surface of the protein that aid in binding the substrates/inhibitors. The binding sites in the target structure were predicted by using the Flood-filling algorithm embedded in Discovery Studio 2.0. A grid resolution of 0.50 Å which is an indication of grid spacing and minimum number of 100 grid points were used for this analysis.

### Screening of analogs

Benzocaine, a local anesthetic commonly used for topical

anesthesia of mucous membranes before endoscopic procedures,<sup>[44]</sup> was used as the parent compound to screen analogs. Pubchem database, a public molecular information repository of the National Institutes of Health Roadmap Initiative,<sup>[45]</sup> and Zinc database, a free database of commercially available compounds for virtual screening, were used for analog screening.<sup>[46]</sup> Molecules in these databases are annotated by molecular property. These include molecular weight, number of rotatable bonds, calculated LogP, number of hydrogen-bond donors, number of hydrogen-bond acceptors, number of chiral centers, number of chiral double bonds (*E/Z* isomerism), polar and apolar desolvation energy (in kcal mol<sup>-1</sup>), net charge, and number of rigid fragments. The molecular properties help in filtering the irrelevant molecules by restricting the search by setting preferable values.

### Pharmacokinetic and pharmacodynamic profiling of screened analogs

Preclinical ADME/Tox studies help in ruling out false positives and identify the most potential drug candidates with appropriate kinetic and dynamic properties.<sup>[47]</sup> For this reason, all the analogs screened from Pubchem compound database and Zinc database were subjected to ADME/T property calculations using the ADME and Topkat modules of Discovery studio. Kinetic properties were estimated in terms of absorption, solubility, hepatotoxicity, cytochrome p450 binding, and its ability to cross blood–brain barrier were analyzed. Toxicity profiles were computationally predicted based on Ames carcinogenicity and NTP carcinogenicity tests. The molecules which were proven to be potentially drug-like were ultimately considered as potential lead molecules for the docking study.

### Pharmacophore modeling

A pharmacophore is defined as the 3D structural features that illustrate how a ligand molecule can interact with a target receptor in a specific binding site. A common-feature pharmacophore model was derived with the HipHop module of catalyst for the drugs that were validated by pharmacokinetics and toxicity studies. The 'Principal' value and 'MaxOmitFeat' value for the compounds were set to 1 and 0, respectively. Diverse conformational models for each compound were generated using the 'best conformational analysis' method with an energy threshold of 20 kcal/mol above the global energy minimum for conformation searching. The maximum number of conformers for each molecule was specified as 250 to ensure maximum coverage of the conformational space. Five kinds of features including hydrogen-bond acceptor (HBA), hydrogen-bond donor (HBD), hydrophobic group (HYD), and positive ionizable (P) and ring aromatic (R) features were selected to initiate the pharmacophore hypotheses generation process.

## Docking

The LigandFit module in Discovery Studio was used to perform the docking, based on shape-based searching and Monte Carlo methods. While docking, the variable trials Monte Carlo conformation was applied where the number of steps depends on the number of rotatable bonds in the ligand. By default, the torsions number is 2, the number of trials is 500 and the maximum successive failure is 120.<sup>[48]</sup> The docking poses were evaluated based on dock scores and hydrogen bonding with the binding site residues. The scoring system included Ligscore, Piecewise linear potential (PLP), Jain, Potential Mean Force (PMF), and dock score.

## RESULTS AND DISCUSSION

### Binding site analysis

The 3D structure of Ricin A chain was retrieved from PDB and was prepared for docking by removing all hetero atoms and solvent molecules associated with the protein. The structure of the protein in its secondary structural view is shown in Figure 1. The flood filling algorithm used for predicting the cavities identified seven binding sites within the protein. Based on the area and volume of the cavities the largest binding site having a volume of 86.625 was used as the target site for docking. A site sphere with a radius of 7.2 surrounding the binding site was created to identify the residues present within the binding site perimeter. The site included around 16 residues and was identified to be Asn78, Ala79, Tyr80, Val81, Gly121, Asn122, Tyr123, Leu126, Ile169, Ile172, Gln173, Ser176, Glu177, Arg180, Glu208, and Trp211. The binding site enclosed within the sphere and the corresponding residues are depicted in Figure 2. The binding site included all the functional residues of ricin namely Tyr80, Tyr123, Glu177, and Arg180 which are used for various purposes such as hydrolysis of adenine ring, stabilization of carboxonium ion, substrate binding, etc.<sup>[43]</sup> and thus is identified to be the most desired site for inhibition.<sup>[49-52]</sup> The drugs were limited to this search space during the docking process.

### Screening and filtering analogs for docking

Taking into consideration the toxicity of ricin on the different organs chiefly the nervous system, the drug benzocaine [Figure 3] was used as reference to screen analogs from Pubchem and Zinc databases. Benzocaine is used as an active ingredient in many drugs and ointment. The pharmacological effect of benzocaine imparted through its structure was used as a base to identify similar compounds that could mimic its structural and functional property. About 66 analogs that more closely resembled the reference drug were selected and their 3D structures are displayed in Figure 4. The analogs were further subjected to filtering by ADME and toxicity studies to identify the

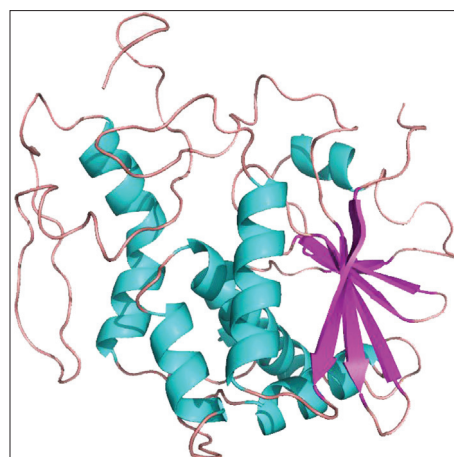


**Figure 1:** Molecular structure of Ricin. The figure displays the 3D structure of ricin in the secondary structural view.

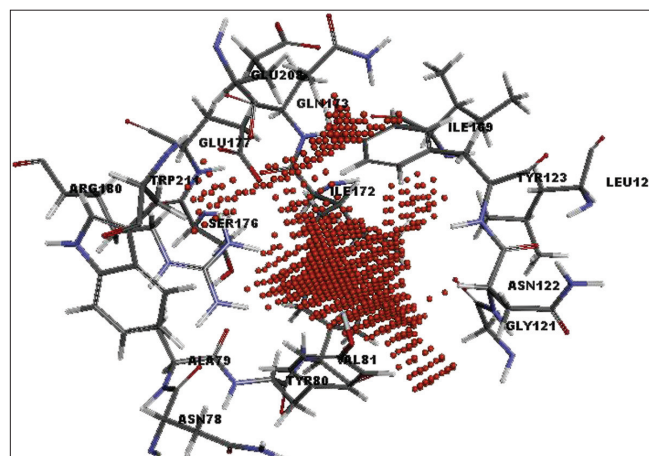


**Figure 2:** Binding site predicted using the flood filling algorithm. The binding site is shown as orange spheres, with the surrounding residues in atom coloring indicating carbon (grey), hydrogen (white), nitrogen (blue), and oxygen (red). The amino acids are labeled with their triple letter codes and position.

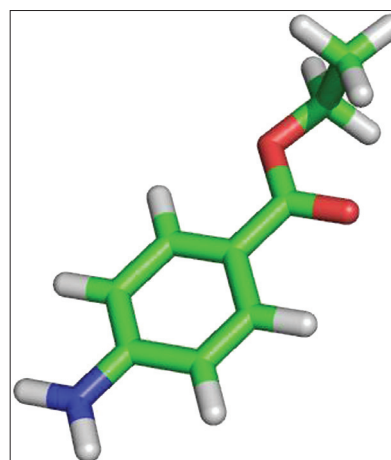


**Figure 3:** Structure of benzocaine. The structure of benzocaine retrieved from Drugbank. Atom colors represent carbon (green), hydrogen (white), nitrogen (blue), and oxygen (red).

**Table 1: ADME and toxicity predictions for the screened analogs**

Molecule	BBB	Absorption	Solubility	Hepatotoxicity	CYPD6	PPB	Carcinogenicity
Molecule 1	3	0	4	0	0	0	False
Molecule 2	3	0	4	0	0	0	False
Molecule 3	3	0	3	1	0	0	False
Molecule 4	3	0	4	0	0	0	False
Molecule 5	3	0	3	1	0	0	False
Molecule 6	3	0	4	1	0	0	False
Molecule 7	2	0	3	0	1	0	False
Molecule 8	3	0	4	0	0	0	False
Molecule 9	3	0	3	1	0	0	False
Molecule 10	3	0	4	0	0	0	False
Molecule 11	3	0	3	1	0	0	False
Molecule 12	3	0	4	0	0	0	False
Molecule 13	3	0	3	0	0	0	False
Molecule 14	3	0	4	1	0	0	False
Molecule 15	2	0	3	0	0	0	False
Molecule 16	3	0	3	1	0	0	False
Molecule 17	3	0	3	1	1	0	False
Molecule 18	3	0	3	0	0	0	False
Molecule 19	3	0	4	1	0	0	False
Molecule 20	3	0	3	1	1	0	False
Molecule 21	3	0	4	1	0	0	False
Molecule 22	3	0	3	0	0	0	False
Molecule 23	3	0	4	0	0	0	False
Molecule 24	3	0	4	0	0	0	False
Molecule 25	3	0	4	0	0	0	False
Molecule 26	3	0	4	1	0	0	False
Molecule 27	3	0	3	0	0	0	False
Molecule 28	2	0	3	1	0	2	False
Molecule 29	3	0	4	1	0	0	False
Molecule 30	3	0	3	1	0	0	False
Molecule 31	3	0	4	0	0	0	False
Molecule 32	3	0	3	0	0	2	False
Molecule 33	3	0	3	1	0	2	False
Molecule 34	3	0	4	1	0	0	False
Molecule 35	3	0	3	1	0	0	False
Molecule 36	3	0	4	0	0	0	False
Molecule 37	3	0	3	1	0	0	False
Molecule 38	2	0	3	1	1	0	False
Molecule 39	2	0	2	0	1	1	False
Molecule 40	2	0	3	1	0	1	False
Molecule 41	3	0	4	0	0	0	False
Molecule 42	4	0	4	0	0	0	False
Molecule 43	3	0	4	1	1	0	False
Molecule 44	4	0	4	1	0	0	False
Molecule 45	2	0	2	1	0	0	False
Molecule 46	3	0	4	1	0	0	False
Molecule 47	3	0	3	1	0	0	False
Molecule 48	3	0	3	0	0	0	False
Molecule 49	4	0	4	1	0	0	False
Molecule 50	2	0	3	1	0	0	False
Molecule 51	3	0	3	0	0	2	False
Molecule 52	2	0	3	0	0	1	False
Molecule 53	2	0	3	0	0	2	False
Molecule 54	3	0	3	0	0	2	False
Molecule 55	3	0	4	1	0	0	False
Molecule 56	3	0	3	0	0	0	False
Molecule 57	3	0	3	0	0	2	False
Molecule 58	3	0	3	1	1	0	False
Molecule 59	4	0	4	0	0	0	False
Molecule 60	3	0	4	0	0	0	False
Molecule 61	2	0	3	0	0	2	False
Molecule 62	2	0	3	0	0	2	False
Molecule 63	3	0	3	0	0	0	False
Molecule 64	2	0	2	0	0	0	False
Molecule 65	3	0	3	0	0	0	False
Molecule 66	3	0	3	0	0	0	False

The analogs with appropriate kinetic and toxicity profiles are shaded in grey.



Figure 4: Analogs screened from Pubchem and Zinc databases.

Molecule	IUPAC name	Molecular weight (g/mol)	Chemical formula
Molecule 7	heptyl 3-(methanesulfonamido) benzoate	313.412	$C_{15}H_{23}NO_4S$
Molecule 52	propyl 3-aminobenzoate	179.216	$C_{10}H_{13}NO_2$
Molecule 53	butyl 3-aminobenzoate	193.242	$C_{11}H_{15}NO_2$
Molecule 61	butyl 3-aminobenzoate hydrochloride	229.703	$C_{11}H_{16}ClNO_2$
Molecule 62	3-methylbutyl 3-aminobenzoate	207.269	$C_{12}H_{17}NO_2$
Molecule 64	3-[(3-methoxy-3-oxopropyl) sulfonylamino]benzoate	286.281	$C_{11}H_{12}NO_6S$

most potential drug-like compounds. The ADME/T properties such as solubility, absorption, plasma protein binding, blood–brain barrier and cytochrome binding and carcinogenicity profiles for all the 66 analogs are given in Table 1. The suitable analogs were selected by comparing the kinetic and toxicity values with the reference values given by the program. The analogs 7, 52, 53, 61, 62, and 64 were identified to be the most potential molecules showing

Table 3: Distances between the pharmacophore features

Features	HBD		HBA		HYD	
	IP	PP	IP	PP		
HBD	IP	0	3.0	5.97	8.84	7.0
	PP	–	0	8.86	9.88	4.94
HBA	IP	–	–	0	3.0	6.47
	PP	–	–	–	0	8.85
HYD	–	–	–	–	–	0

This table shows the distances computed among each of the pharmacophore features. HBD, hydrogen bond donor; HBA, hydrogen bond acceptor; HYD, hydrophobe; IP, internal point; PP, projection point.

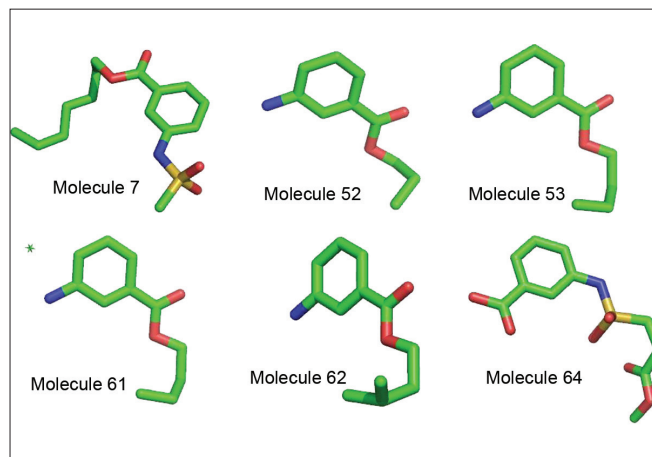
no toxicity and more drug-like property. The details of the six selected analogs are given in Table 2, and their 3D structures are represented in Figure 5.

### Pharmacophore modeling

The six most potential analogs predicted from the ADME/T studies were selected for pharmacophore modeling which is one of the most powerful methods to categorize and identify key features from a group of molecules. The pharmacophore, predicted to identify the common functional moieties for the six analogs, showed a hydrogen bond donor, hydrogen bond acceptor, and a

**Table 4: Dock scores computed for different scoring functions**

Drugs	Ligscore 1	Ligscore 2	PLP1	PLP2	Jain	PMF	Dockscore
Mol 7	3.04	4.62	49.36	49.79	-1.91	83.83	46.632
Mol 52	2.79	4.85	70.97	69.5	1.64	94.1	38.518
Mol 53	2.67	4.6	68.74	67.05	0	92.16	41.315
Mol 62	3.03	4.94	75.14	73.59	0.28	103.69	42.3
Mol 64	4.58	5.14	77.66	74.69	1.09	105.3	59.459

**Figure 5:** Analogs screened from ADME/Tox studies.

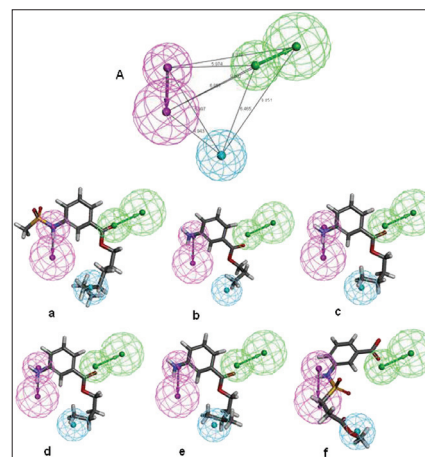
hydrophobe with a maximum fit value of 3 for analog 7. The aligned molecule with the pharmacophore for each of the six analogs is shown in Figure 6. The distances between each of the pharmacophore features were predicted and are presented in Table 3. This pharmacophore model will provide a new insight to design novel molecules that can inhibit the function of the target and will be useful in drug discovery strategies.

Table 3 shows the distances computed between each of the pharmacophore features. Abbreviations denote HBD, hydrogen bond donor; HBA, hydrogen bond acceptor; HYD, hydrophobe; IP, Internal point; and PP, projection point.

### Interaction studies

The six selected analogs were docked into the binding site of the receptor using Ligand fit protocol. The docking run generated 10 poses for each of the analog. The ligscore, Jain, PLP and PMF scoring functions were used to identify the best docked pose. Of the six molecules docked analog 61 failed to interact with the receptor and thus did not generate any poses. The dock scores computed by the different scoring functions for the remaining five analogs are tabulated in Table 4.

The docked poses for each of the drugs and their interacting residues with distances are illustrated in Figure 6. The stability of the docked poses was evaluated by determining the hydrogen bonding between the receptor

**Figure 6:** Common feature pharmacophore models generated by Hiphop algorithm. (A) The common feature pharmacophore predicted by aligning the drugs. The alignment of the features with the (a) analog 7, (b) analog 52, (c) analog 53, (d) analog 61, (e) analog 62, and (f) analog 64 is also shown.

and ligand. The interaction pattern analyzed based on the functional residues indicated that all five analogs formed hydrogen bonds with Tyr80 [Figure 7a & 7c], analogs 62 [Figure 7d], and 64 [Figure 7e] additionally formed bonds with Tyr108, only analog 52 [Figure 7b] formed hydrogen bonds with Tyr 123. None of the analogs interacted with Glu177 of the functional residues. The dock score for all the docked drugs showed analog 64 to have the highest dock score of 59.459 and formed stable interaction with the residues Tyr80, Arg180, and Val81. From the overall docking, we identified analog 64 to be the best interacting compound based on the dock score and bonded interactions with the functional residues of the target protein.

## CONCLUSION

Virtual screening has become one of the significant approaches in identifying potential compounds in drug designing. This method was adopted in our work to identify compounds that can inhibit/block the function of ricin, a deadly toxin. We identified 66 analogs based on the functional and structural aspects of benzocaine, an analgesic. A computational docking study was carried out with the 66 analogs. From the results, we were able to identify one such molecule (Molecule 64: 3-[(3-methoxy-

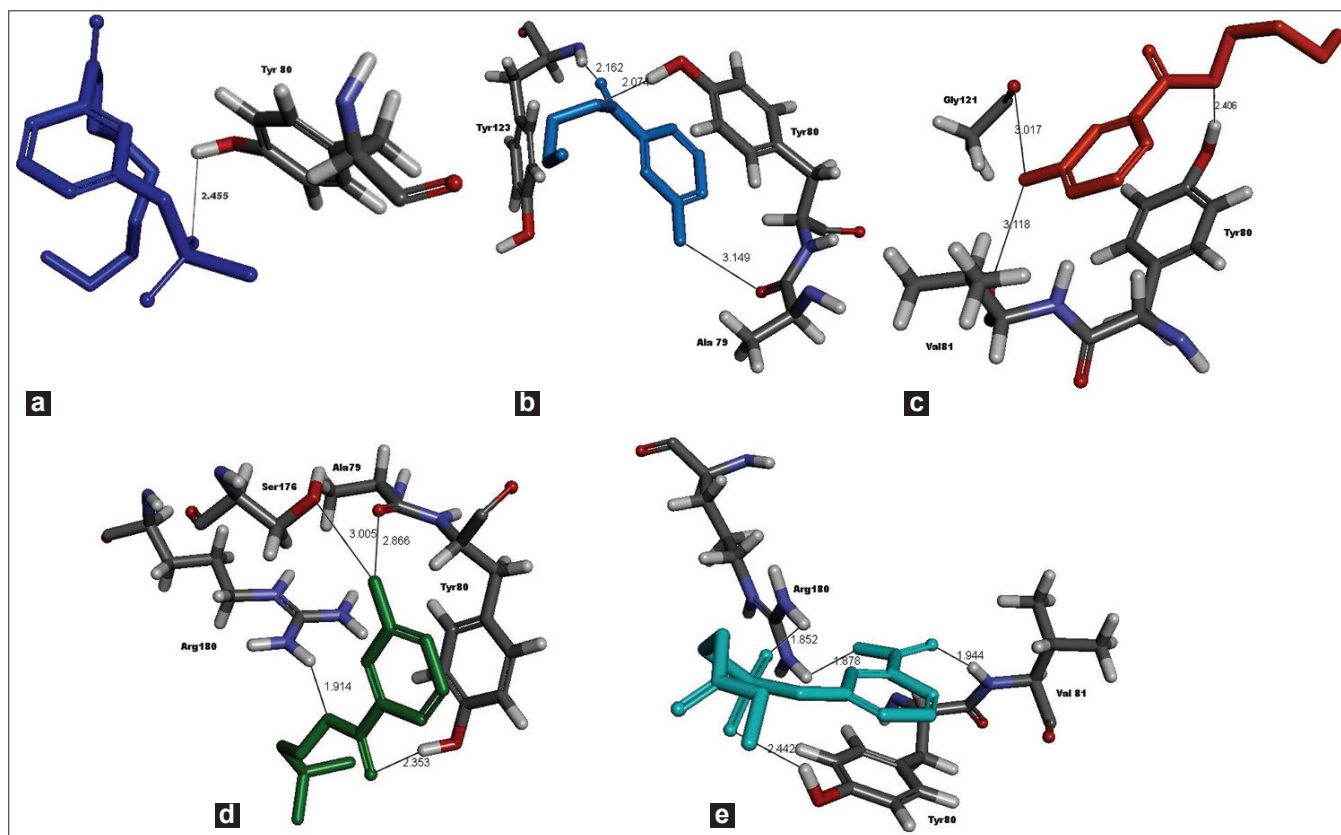


**Figure 7:** Interactions of the analogs at the ricin binding site. (a) Analog 7 showing interaction with Tyr80 with distance of 2.455 Å. (b) Analog 52 showing interactions with Ala79 (3.149 Å), Tyr80 (2.074 Å), and Tyr123 (2.162 Å). (c) Analog 53 showing interactions with Tyr80 (2.406 Å), Val81 (3.118 Å), and Gly121 (3.017 Å). (d) Analog 62 showing interactions with Ala79 (2.866 Å), Tyr80 (2.353 Å), Ser176 (3.005 Å), and Arg 180 (1.914 Å). (e) Analog 64 showing interactions with Tyr80 (2.442 Å), Val81 (1.944 Å), Arg180 (2 bonds with 1.852 Å and 1.878 Å).

3-oxopropyl)sulfonylamino] benzoate) that had a good binding toward the functional residues of ricin. The pharmacokinetic and dynamic parameters of the analog were also studied *in silico* and were proven to have a drug-like property. The work can be further evaluated experimentally to study the receptor–ligand interactions *in vivo*. The pharmacophore features of the drugs provided suggests the key functional groups that can aid in the design and synthesis of more potential inhibitors.

## ACKNOWLEDGMENTS

The authors are grateful and thank the management of Sathyabama University for providing the cluster computing lab facility to carry out this study. The authors also thank the anonymous reviewers for their valuable comments and suggestions.

## REFERENCES

- Audi J, Belson M, Patel M, Schier J, Osterloh J. Ricin poisoning: A comprehensive review. *JAMA* 2005;294:2342-51.
- Balint GS. Ricin--2004. *Orv Hetil* 2004;145:2379-81.
- Schep LJ, Temple WA, Butt GA, Beasley MD. Ricin as a weapon of mass terror--Separating fact from fiction. *Environ Int* 2009;35:1267-71.
- Spivak L, Hendrickson RG. Ricin. *Crit Care Clin* 2005;21: 815-24.
- Musshoff F, Madea B. Ricin poisoning and forensic toxicology. *Drug Test Anal* 2009;1:184-91.
- Papaloucas M, Papaloucas C, Stergioulas A. Ricin and the assassination of Georgi Markov. *Pak J Biol Sci* 2008;11:2370-1.
- Korcheva V, Wong J, Corless C, Iordanov M, Magun B, Administration of ricin induces a severe inflammatory response via nonredundant stimulation of ERK, JNK, and P38 MAPK and provides a mouse model of hemolytic uremic syndrome. *Am J Pathol* 2005;166:323-39.
- Strocchi P, Dozza B, Pecorella I, Fresina M, Campos E, Stirpe F. Lesions caused by ricin applied to rabbit eyes. *Invest Ophthalmol Vis Sci* 2005;46:1113-6.
- Sharma RD, Veerpathran AR, Dakshinamoorthy G, Sahare KN, Goswami K, Reddy MV. Possible implication of oxidative stress in anti filarial effect of certain traditionally used medicinal plants *in vitro* against *Brugia malayi* microfilariae. *Pharmacogn Res* 2010;2:350-4.
- Nagy M. Ricin-a plant toxin with potential therapeutic use. *Ceska Slov Farm* 2004;53:131-40.
- Lim H, Kim HJ, Cho YS. A case of ricin poisoning following ingestion of Korean castor bean. *Emerg Med J* 2009;26:301-2.
- Leshin J, Danielsen M, Credle JJ, Weeks A, O'Connell KP, Dretchen K. Characterization of ricin toxin family members from *Ricinus communis*. *Toxicon* 2010;55:658-61.



13. Lindauer M, Wong J, Magun B. Ricin toxin activates the NALP3 inflammasome. *Toxins (Basel)* 2010;2:1500-14.
14. Ramprasad R, Bandopadhyay R. Future of *Ricinus communis* after completion of the draft genome sequence. *Curr Sci* 2010;1315-6.
15. Griffiths GD, Phillips GJ, Holley J. Inhalation toxicology of ricin preparations: Animal models, prophylactic and therapeutic approaches to protection. *Inhalational Toxicol* 2007;19:873-87.
16. Kitaoka Y. Involvement of the amino acids outside the active-site cleft in the catalysis of ricin A chain. *Eur J Biochem* 1998;257:255-62.
17. Riccobono F, Fiani ML. Mannose receptor dependent uptake of ricin A1 and A2 chains by macrophages. *Carbohydr Res* 1996;282:285-92.
18. Sandvig K, van Deurs B. Endocytosis and intracellular transport of ricin: Recent discoveries. *FEBS Lett* 1999;452:67-70.
19. Sandvig K, Grimmer S, Lauvrak SU, Torgersen ML, Skretting G, van Deurs B, *et al.* Pathways followed by ricin and Shiga toxin into cells. *Histochem Cell Biol* 2002;117:131-41.
20. Wesche J. Retrograde transport of ricin. *Int J Med Microbiol* 2002;291:517-21.
21. Lord MJ, Jolliffe NA, Marsden CJ, Pateman CS, Smith DC, Spooner RA, *et al.* Ricin: Mechanisms of cytotoxicity. *Toxicol Rev* 2003;22:53-64.
22. Liu L, Gao H, Li J, Dong Y, Liu N, Wan J, *et al.* Analysis of intestinal injuries induced by ricin *in vitro* using SPR technology and MS identification. *Int J Mol Sci* 2009;10:2431-9.
23. Simmons BM, Stahl PD, Russell JH. Mannose receptor-mediated uptake of ricin toxin and ricin A chain by macrophages. Multiple intracellular pathways for a chain translocation. *J Biol Chem* 1986;261:7912-20.
24. Battelli MG, Musiani S, Monti B, Buonamici L, Sparapani M, Contestabile A, *et al.* Ricin toxicity to microglial and monocytic cells. *Neurochem Int* 2001;39:83-93.
25. Nagatsuka T, Uzawa H, Ohsawa I, Seto Y, Nishida Y. Use of lactose against the deadly biological toxin ricin. *ACS Appl Mater Interfaces* 2010;2:1081-5.
26. Spilberg B, Van Meer G, Sandvig K. Role of lipids in the retrograde pathway of ricin intoxication. *Traffic* 2003;4:544-52.
27. Pandey G, Madhuri S. Some medicinal plants as natural anticancer agents. *Pharmacogn Rev* 2009;3:259-63.
28. Rao PV, Jayaraj R, Bhaskar AS, Kumar O, Bhattacharya R, Saxena P, *et al.* Mechanism of ricin-induced apoptosis in human cervical cancer cells. *Biochem Pharmacol* 2005;69:855-65.
29. Gan YH, Peng SQ, Liu HY. Molecular mechanism of apoptosis induced by ricin in HeLa cells. *Acta Pharmacol Sin* 2000;21:243-8.
30. Zou LB, Zhan JB. Purification and anti-cancer activity of ricin. *Zhejiang Da Xue Xue Bao Yi Xue Ban* 2005;34:217-9.
31. Schnell R, Borchmann P, Staak JO, Schindler J, Ghetie V, Vitetta ES, *et al.* Clinical evaluation of ricin A-chain immunotoxins in patients with Hodgkin's lymphoma. *Ann Oncol* 2003;14:729-36.
32. Engert A, Sausville EA, Vitetta E. The emerging role of ricin A-chain immunotoxins in leukemia and lymphoma. *Curr Top Microbiol Immunol* 1998;243:13-33.
33. Thakur L, Ghodasra U, Patel N, Dabhi M. Novel approaches for stability improvement in natural medicines. *Pharmacogn Rev* 2011;5:48-54.
34. Sun J, Pohl EE, Krylova OO, Krause E, Agapov II, Tonevitsky AG, *et al.* Membrane destabilization by ricin. *Eur Biophys J* 2004;33:572-9.
35. Marsden CJ, Knight S, Smith DC, Day PJ, Roberts LM, Phillips GJ, *et al.* Insertional mutagenesis of ricin A chain: A novel route to an anti-ricin vaccine. *Vaccine* 2004;22:2800-5.
36. Olson MA, Carra JH, Roxas-Duncan V, Wannemacher RW, Smith LA, Millard CB. Finding a new vaccine in the ricin protein fold. *Protein Eng Des Sel* 2004;17:391-7.
37. Dertzbaugh MT, Rossi CA, Paddle BM, Hale M, Poretski M, Alderton MR. Monoclonal antibodies to ricin: *In vitro* inhibition of toxicity and utility as diagnostic reagents. *Hybridoma (Larchmt)* 2005;24:236-43.
38. Legler PM, Brey RN, Smallshaw JE, Vitetta ES, Millard CB. Structure of RiVax: A recombinant ricin vaccine. *Acta Crystallogr D Biol Crystallogr* 2011;67:826-30.
39. Bai Y, Watt B, Wahome PG, Mantis NJ, Robertus JD. Identification of new classes of ricin toxin inhibitors by virtual screening. *Toxicol* 2010;56:526-34.
40. Mishra V, Prasad CV. Ligand based virtual screening to find novel inhibitors against plant toxin Ricin by using the ZINC database. *Bioinformation* 2011;7:46-51.
41. Khan AH, Prakash A, Kumar D, Rawat AK, Srivastava R, Srivastava S. Virtual screening and pharmacophore studies for f1ase inhibitors using Indian plant anticancer compounds database. *Bioinformation* 2010;5:62-6.
42. Kumar RB, Shanmugapriya B, Thiyagesan K, Kumar SR, Xavier SM. A search for mosquito larvicidal compounds by blocking the sterol carrying protein, AeSCP-2, through computational screening and docking strategies. *Pharmacognosy Res* 2010;2:247-53.
43. Monzingo AF, Robertus JD. X-ray analysis of substrate analogs in the ricin A-chain active site. *J Mol Biol* 1992;227:1136-45.
44. Sachdeva R, Pugada JG, Casale LR, Meizlish JL, Zarich SW. Benzocaine-induced methemoglobinemia: A potentially fatal complication of transesophageal echocardiography. *Tex Heart Inst J* 2003;30:308-10.
45. Xie XQ. Exploiting Pubchem for virtual screening. *Expert Opin Drug Discov* 2010;5:1205-20.
46. Irwin JJ, Shoichet BK. ZINC—A free database of commercially available compounds for virtual screening. *J Chem Inf Model* 2005;45:177-82.
47. Ekins S, Nikolsky Y, Nikolskaya T. Techniques: Application of systems biology to absorption, distribution, metabolism, excretion and toxicity. *Trends Pharmacol Sci* 2005;26:202-9.
48. Patil R, Das S, Stanley A, Yadav L, Sudhakar A, Varma AK. Optimized hydrophobic interactions and hydrogen bonding at the target-ligand interface leads the pathways of drug-designing. *PLoS One* 2010;5:e12029.
49. Robertus JD, Yan X, Ernst S, Monzingo A, Worley S, Day P, *et al.* Structural analysis of ricin and implications for inhibitor design. *Toxicol* 1996;34:1325-34.
50. Ramalingam TS, Das PK, Podder SK. Identification of the adenine binding site in the ricin toxin –a chain by fluorescence, cd, and electron spin resonance spectroscopy. *Biopolymers* 1993;33:1687-94.
51. Schlossman D, Withers D, Welsh P, Alexander A, Robertus J, Frankel A. Role of glutamic acid 177 of the ricin toxin A chain in enzymatic inactivation of ribosomes. *Mol Cell Biol* 1989;9:5012-21.
52. Frankel A, Welsh P, Richardson J, Robertus JD. Role of arginine 180 and glutamic acid 177 of ricin toxin A chain in enzymatic inactivation of ribosomes. *Mol Cell Biol* 1990;10:6257-63.

**Cite this article as:** Kumar RB, Suresh MX. A computational perspective of molecular interactions through virtual screening, pharmacokinetic and dynamic prediction on ribosome toxin A chain and inhibitors of *Ricinus communis*. *Phcog Res* 2012;4:2-10.

**Source of Support:** Nil, **Conflict of Interest:** None declared.